# AIR–SEA EXCHANGE IN HURRICANES

## Synthesis of Observations from the Coupled Boundary Layer Air–Sea Transfer Experiment

BY PETER G. BLACK, ERIC A. D'ASARO, WILLIAM M. DRENNAN, JEFFREY R. FRENCH, PEARN P. NIILER, THOMAS B. SANFORD, ERIC J. TERRILL, EDWARD J. WALSH, AND JUN A. ZHANG

Combining airborne remote, in situ, and expendable probe sensors with air-deployed ocean platforms provides a strategy for expanding knowledge of illusive high-wind air–sea fluxes in difficult-to-predict storms.

The CBLAST (see Table 1 for a list of the acronyms and their expansions used herein) experiment was conducted during 2000–05 to improve our fundamental understanding of physical processes at the air–sea interface. We focus here on the CBLAST-Hurricane component, which included experimental observations of the air–sea exchange process in high winds suitable for improving hurricane-track and intensity model physics. Other CBLAST activities focused on low-wind dynamics (Edson et al. 2007) and coupled modeling of hurricanes (Chen et al. 2007).

Energy exchange at the air–sea interface is one of the three major physical processes governing hurricane intensity change; the others are environmental interactions with surrounding large-scale features in the atmosphere, and internal dynamics such as eyewall replacement cycles and cloud microphysics. The air–sea exchange of heat, moisture, and momentum determines how hurricanes gain their strength and intensity from the ocean. This has become an extremely important problem over the past several years because it appears that we have entered a new era with a greater number of hurricanes (Goldenberg 2001). During 2004–05, an increase in the number of major hurricane landfalls has ocurred. While efforts to forecast hurricane tracks have improved greatly over the past 15 years, our ability to forecast hurricane intensity has shown little skill (DeMaria et al. 2005). With more hurricane threats on the U.S. and Caribbean coastlines, the effort to improve hurricane intensity forecasting has taken on a greater urgency. The mitigation actions that are taken by emergency management officials; local, state, and federal governments; and private industry all depend on predictions

**AFFILIATIONS:** BLACK—NOAA/AOML Hurricane Research Division, Miami, Florida; D'ASARO AND SANFORD—Applied Physics Laboratory, University of Washington, Seattle, Washington; DRENNAN AND ZHANG—Rosenstiel School of Marine and Atmospheric Science, University of Miami, Miami, Florida; FRENCH—Department of Atmospheric Science, University of Wyoming, Laramie, Wyoming; NIILER AND TERRILL—Scripps Institution of Oceanography, University of California, San Diego, La Jolla, California; WALSH—NASA Goddard Space Flight Center at NOAA Earth System Research Laboratory, Boulder, Colorado.
**CORRESPONDING AUTHOR:** Peter G. Black, NOAA/AOML Hurricane Research Division, Miami, FL 33149
E-mail: Peter.Black@noaa.gov

*The abstract for this article can be found in this issue, following the table of contents.*
DOI:10.1175/BAMS-88-3-357

In final form 14 July 2006

| Table 1. List of acronyms. | | | |
|---|---|---|---|
| ADOS | Autonomous Drifting Ocean Stations | NRL | Naval Research Laboratory |
| AFRC | Air Force Reserve Command | OAR | Office of Oceanic and Atmospheric Research |
| AMP | Applied Marine Physics | OHC | Ocean heat content |
| AOC | Aircraft Operations Center | ONR | Office of Naval Research |
| AOML | Atlantic Oceanographic and Meteorological Laboratory | ORA | Office of Research and Applications |
| APL | Applied Physics Laboratory (University of Washington) | PDA | Particle Doppler Analyzer |
| ARL | Air Resources Laboratory | PHOD | Physical Oceanography Division |
| AXBT | Airborne Expendable Bathythermograph | PI | Principal investigator |
| BAT | Best Aircraft Turbulence (probe) | PBL | Planetary boundary layer |
| CBLAST | Coupled Boundary Layer Air–Sea Transfer | PDA | Particle Doppler Analyzer |
| CIP | Cloud-imaging probe | RSMAS | Rosenstiel School of Marine and Atmospheric Science |
| COAMPS | Coupled Ocean–Atmosphere Mesoscale Prediction System | R/V | Research vessel |
| COARE | Coupled Ocean–Atmosphere Response Experiment | SAR | Synthetic Aperture Radar |
| DOW | Doppler on Wheels | SATCOM | Satellite Communications (system) |
| EM-APEX | Electro-Magnetic Autonomous Profiling Explorer | SBIR | Small Business Innovative Research (program) |
| EMC | Environmental Modeling Center | SCRIPPS | Scripps Institution of Oceanography |
| ENVISAT | Environmental Satellite (European Space Agency) | SFMR | Stepped-Frequency Microwave Radiometer |
| GSFC | Goddard Space Flight Center | SOCD | Satellite Oceanography and Climatology Division |
| HEXOS | Humidity Exchange over the Sea | SOLO | Sounding Oceanographic Lagrangian Observer |
| HRD | Hurricane Research Division | SRA | Scanning Radar Altimeter |
| HWRF | Hurricane Weather Research and Forecasting | SST | Sea surface temperature |
| IWRAP | Integrated Wind and Rain Atmospheric Profiler | STAR | Center for Satellite Applications and Research |
| IOOS | Integrated Ocean Observing System | SVP | Surface Velocity Program |
| JD | Julian Day | TA | Tail (airborne Doppler radar) |
| LF | Lower fuselage | TC | Tropical cyclone |
| MIRSL | Microwave Remote Sensing Laboratory | UCSD | University of California, San Diego |
| MIT | Massachusetts Institute of Technology | UMASS | University of Massachusetts |
| MODIS | Moderate Resolution Imaging Spectroradiometer | UNOLS | University–National Oceanographic Laboratory System |
| NASA | National Aeronautics and Space Administration | USFMR | UMASS Simultaneous Frequency Microwave Radiometer |
| NESDIS | National Environmental Satellite Data Information Service | USWRP | U.S. Weather Research Program |
| NHC | National Hurricane Center | WRS | Weather Reconnaissance Squadron |
| NOAA | National Oceanic and Atmospheric Administration | WSR-88D | Weather Surveillance Radar-1988 Doppler |
| NOGAPS | Navy Operational Global Atmospheric Prediction System | | |

**Table 2a. CBLAST-Hurricane PI Team: functions and observable quantities, instrumentation, and PIs.**

| No. | Function | Instrument | PI | Affiliation |
|---|---|---|---|---|
| 1 | Chief scientist, flight planning, program coordination | All | Peter Black | NOAA/AOML/HRD |
| 2 | Ocean winds lead scientist, surface wind vector, SATCOM, satellite applications | IWRAP | Paul Chang | NOAA/NESDIS/STAR/ SOCD |
| 3 | Dropsondes SST, surface wind speed | GPS sonde, AXBT, SFMR | Peter Black, Eric Uhlhorn | NOAA/AOML/HRD |
| 4 | Sea spray, particle spectrometer | CIP | Chris Fairall | NOAA/ESRL/ETL |
| 5 | Sea spray, particle velocimeter | PDA | William Asher | University of Washington APL |
| 6 | Extreme wind surface flux, theory | Dropsonde | Kerry Emanuel | MIT |
| 7 | Surface waves | SRA | Ed Walsh | NASA Goddard |
| 8 | Momentum, sensible heat flux | BAT | Jeff French | NOAA/ARL; University of Wyoming |
| 9 | Moisture flux | LI-COR | William Drennan | University of Miami/ RSMAS/AMP |
| 10 | Surface wind vector, continuous PBL wind profiles | IWRAP, USFMR | Stephen Frasier, James Carswell, Daniel Esteban, Rob Contreras | UMASS MIRSL |
| 11 | Surface wave breaking, foam coverage | Scripps VIS, IR camera | Ken Melville, Eric Terrill | UCSD/SCRIPPS |

**Table 2b. CBLAST-Hurricane PI team: functions and observable quantities, instrumentation, and drifter float component.**

| No. | Function | Instrument | PI | Affiliation |
|---|---|---|---|---|
| 1 | Ocean mixing, gas exchange | Lagrangian floats | Eric D'Asaro | University of Washington APL |
| 2 | Ocean current, temperature, and salinity profiling | EM-APEX floats | Tom Sanford | University of Washington APL |
| 3 | Ocean acoustics, surface waves, ocean temperature profiles | SOLO floats | Eric Terrill | UCSD/SCRIPPS |
| 4 | SST, surface wind vector, ocean acoustics, surface air pressure | SVP/ADOS drifters | Peter Niiler, William Scuba, Jan Morzel | UCSD/SCRIPPS |
| 5 | Satellite ocean heat content, buoy archive | Satellite altimeters | Gustavo Goni | NOAA/AOML/PHOD |

of intensity thresholds at and near landfall. In response to this need for improved hurricane intensity forecasts, the ONR initiated the CBLAST program to complement ongoing hurricane intensity research programs in universities and government laboratories, such as the HRD.

The resulting CBLAST-Hurricane experiment became a cooperative undertaking between the ONR, NOAA's OAR, HRD, AOC, including its USWRP, and the U.S. AFRC's 53rd WRS. ONR provided support for 17 PIs (see Table 2) from universities and government laboratories. NOAA provided aircraft flight hour support for two WP-3D research aircraft, expendable probes, and Hurricane Field Program infrastructure. AFRC, through the 53rd WRS, provided infrastructure support, specialized expertise in air deployment of large platforms, and WC-130J and C-130J aircraft support. The observational strategies and initial results of this effort are described in the following pages.

The overarching goal of CBLAST was to provide a new physical understanding that would improve forecasting of hurricane intensity change with the new suite of operational models now undergoing testing and evaluation at the NRL and at NOAA's EMC. CBLAST focused an intensive effort on observing air–sea interaction processes within hurricanes because of the

recognized lack of knowledge of the physics of air–sea exchange at winds above gale force. Prior to CBLAST, no in situ air–sea flux measurements existed at wind speeds above 22 m $s^{-1}$. Parameterization schemes used to approximate air–sea transfer at hurricane wind speeds were simply an extrapolation of low-wind measurements with the assumption that the physical processes were the same, despite clear evidence to the contrary! A key goal of CBLAST was to extend the range of observations for exchange coefficients of momentum, heat, and moisture across the air–sea interface to hurricane-force winds, and above.

**CBLAST CONCEPT AND OBSERVATION PLAN.** The CBLAST experimental design consisted of two major observational components: 1) airborne in situ and remote sensing instrumentation flown into hurricanes by the two NOAA WP-3D aircraft, and 2) air-deployed surface-drifting buoys and subsurface-profiling floats. This was intended to provide a mix of "snapshots" of inner-core hurricane conditions each day over a 2–4-day period, together with a continuous time series of events at particular ocean locations. A third component, available based on operational needs, consisted of the hurricane synoptic surveillance program designed for improved track forecasting. It provided, on occasion, concurrent high-level NOAA G-IV jet aircraft flights in the hurricane environment, deploying GPS dropsondes to profile the steering currents and significant synoptic features, in addition to reconnaissance flights within the hurricane's inner core from the WC-130H aircraft, operated by AFRC's 53rd WRS. Polar-orbiting and geostationary satellite platforms provided additional remote sensing measurements in the hurricane's inner core and environment. This approach provided an overarching database to allow intensity changes from air–sea interaction causes to be separable from those resulting from atmospheric environmental interactions and internal dynamics.

The aircraft component of CBLAST had the following two modules: a) an aircraft stepped-descent module, and b) an inner-core survey module. The former was designed to focus on in situ air–sea flux and spray measurements, while the latter was designed to focus on the large-scale structure, eyewall flux budget measurements, and documentation of internal dynamics. The centerpiece of this effort involved a multisonde sequence of 8–12 GPS dropsondes dropped from coordinated WP-3Ds flying in tandem at different altitudes across the hurricane eyewall and eye. See Fig. 1 for a schematic of a typical flight plan. Each module consisted of several options related to precise experimental patterns dictated by prevailing conditions and available on-station time. For instance, the stepped descents (Fig. 2), designed to probe the hurricane boundary layer down to as low as 70 m above the sea, were only carried out in clear-air conditions between rainbands.

Both modules were complemented with an array of airborne remote and in situ sensors. Air-deployed drifting buoys (drifters) and oceanographic floats (autoprofiling oceanographic radiosondes) were designed to further complement the airborne in situ and remote sensing of the air–sea interface. This drifter–float air-deployment module consisted of arrays of sensors measuring continuous time series of surface and upper-ocean conditions before, during, and after hurricane passage. Together, the aircraft and drifter–float array provided a unique description of air–sea fluxes, and surface wave and upper-ocean conditions in hurricane conditions never before achieved. In a similar fashion, the inner-core survey module provided observations of significant changes

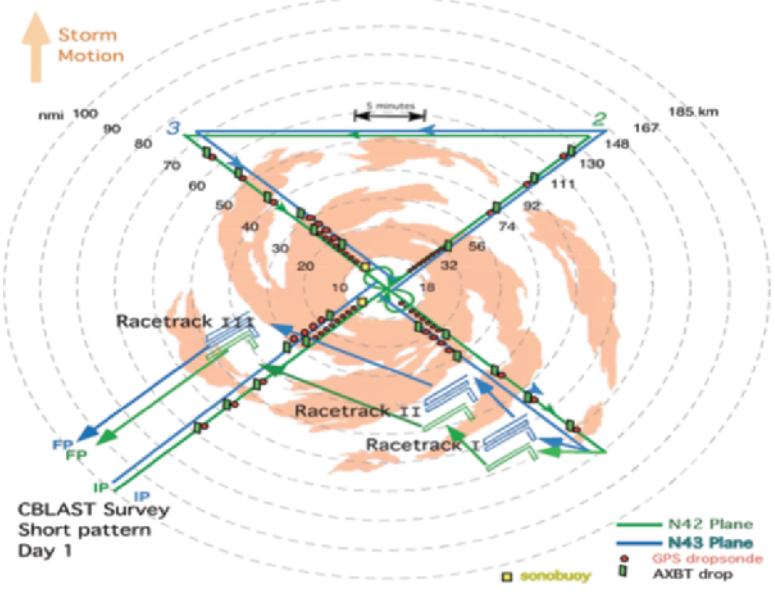


**Fig. 1. CBLAST survey pattern showing planned expendable probe deployments along a "figure 4" pattern relative to the storm's eyewall and rainband features. Location of planned stepped-descent patterns to measure boundary layer fluxes is shown schematically; IP is the initial point in the pattern, and FP is the final point.**

in the inner-core dynamics occurring concurrently with observed air–sea processes.

**CASE STUDIES.** The CBLAST experimental effort began in 2000 with the development of seven new airborne instrument systems, three new oceanographic float designs, two drifting buoy designs, the flight pattern strategy, and the air-deployment strategy, including the WC-130J air-deployment certification and air-drop certification of three platform types. The new airborne instrument systems were 1) the BAT probe for fast-response temperature and *u, v,* and *w* wind components, 2) a modified LI-COR fast-response hygrometer, 3) a CIP particle spectrometer, 4) PDA for sea-spray droplet observation, 5) Scripps downward-looking, high-speed visible and infrared videocamera systems for wave-breaking observations, 6) SFMR and USFMR for surface wind speed, and 7) the IWRAP for continuous boundary layer and surface wind vector profiles.

These systems were built in 2001 and flight tested in 2002. Also deployed were the following three existing systems: 1) the TA Doppler radar for boundary layer wind structure, 2) the LF weather radar for hurricane precipitation structure, and 3) the SRA for directional wave spectra. Two storms, Edouard and Isidore, were flown in 2002—the first to test the new stepped-descent flight pattern strategy and the second to test the extended low-level flight pattern for the detection of linear coherent turbulence structures, sometimes referred to as "roll vortex" or "secondary boundary layer" circulations. The CBLAST field program began in earnest in 2003, with the survey flight pattern flown on 6 days by the two NOAA WP-3D aircraft (a total of 12 flights, including 12 stepped-descent patterns) in Hurricanes Fabian and Isabel from a staging base in St. Croix, U.S. Virgin Islands. An additional 10 AFRC WC-130H reconnaissance flights and 3 NOAA G-IV surveillance flights were also flown during this period. An array of 16 drifting buoys and six floats were deployed by the 53rd WRS from a WC-130J aircraft ahead of Hurricane Fabian.

An engine failure due to salt build-up occurred near the end of the sixth flight, which resulted in new safety regulations requiring a chemical engine wash after each flight below 340 m. CBLAST flights in 2004 continued, but were restricted to flight levels above the boundary layer. The CBLAST flights in 2004 were in Hurricanes Frances on 4 days, Ivan on 5 days, and Jeanne on 3 days. The key success in 2004 was the air deployment by the 53rd WRS of 38 drifting buoys (30 Minimet, 8 ADOS) and 14 floats (9 SOLO, 2 Lagrangian, and 3 EM-APEX) ahead of Hurricane Frances on 31 August. All drifters and floats were deployed successfully. The floats were recovered by the UNOLS ship R/V *Cape Hatteras* between 27 September and 4 October, approximately 4 weeks after deployment.

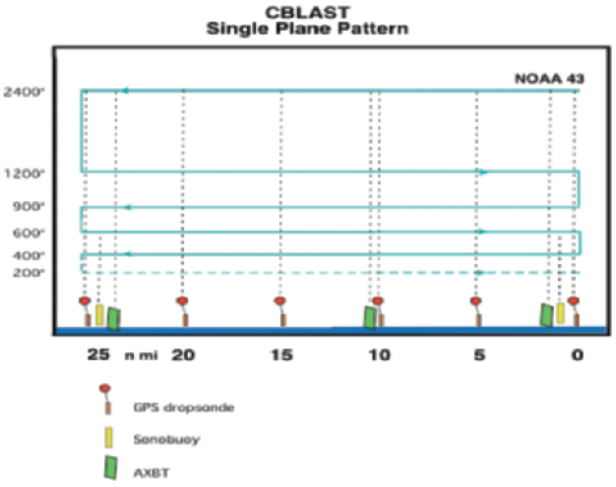


**Fig. 2. Vertical alignment of stepped-descent flight legs along with expendable probe location along the 25-nmi (46 km) leg length.**

**KEY RESULTS FROM THE AIRCRAFT COMPONENT.** *First turbulence measurements in tropical storm- and hurricane-force winds.* The principal results from the aircraft component of CBLAST were the estimation of surface momentum and enthalpy flux from direct eddy correlation measurements using two newly modified airborne instrument packages: the BAT probe and the LI-COR fast-response hygrometer, shown mounted on the WP-3D aircraft in Fig. 3. The results are based on measurements obtained during 15 stepped-descent patterns flown in Hurricanes Fabian and Isabel in 2003 (Fig. 4). These are the first direct-flux measurements ever made in a hurricane and the first in a tropical storm since the gust probe measurements of Moss and Merceret (1976, 1977) and Moss (1978) in the periphery of Tropical Storm Eloise on 17 September 1975, where their estimated surface winds were ~ 20 m $s^{-1}$. [While the authors refer to their measurements in "Hurricane" Eloise, the National Hurricane Center best-track archives (online at www.nhc.noaa.gov/tracks1851to2006_atl.txt) lists the peak surface winds for Eloise on 17 September, 1975, when the center was over Hispañola (Hebert 1976), as tropical storm strength, that is, 22–25 m $s^{-1}$, for the 1800 UTC period of the research flight.] Data from a total of 48 (42) flux runs were used to compute independent estimates of the momentum (humidity)


**Fig. 3. Location of the BAT turbulence probe and LI-COR fast-response humidity probe on the WP-3D aircraft.**

flux. All of the flux runs were flown between 70 and 400 m at an airspeed of close to 113 m $s^{-1}$. Measurements from GPS dropsondes indicate that the top of the hurricane PBL, defined as the top of the constant potential temperature layer, was approximately 500 m (Drennan et al. 2007). Leg lengths ranged from 13 to 55 km, with an average length of 28 km. Fluxes of momentum and humidity were computed using eddy correlation. Profiles of fluxes were analyzed for individual stepped descents. There was no significant height dependence of the humidity flux within the PBL. Momentum flux decreased to only 50%–75% of the surface values near the top of the PBL. Surface friction velocity was computed following Donelan (1990). Ten-meter neutral wind ($U_{10N}$) was taken from leg-averaged measurements (approximately 5 min) from a nadir-pointing SFMR (Uhlhorn and Black 2003; Uhlhorn et al. 2006, manuscript submitted to *Wea. Forecasting,* hereafter UHL06). The drag coefficient ($C_{D10N}$, referred to hereafter as $C_D$) was computed directly from the friction velocity and $U_{10N}$. Surface-saturated specific humidity $q_0$ was estimated based on the SST provided by an infrared radiometer on the aircraft, averaged along the flight track, and corrected for intervening atmospheric absorption. A linear regression line was fit to the measured SST values at each stair-step altitude and the surface value was extrapolated. The difference between the extrapolated surface value and the average value for each flux run was then computed and used to correct the measured SST to the true value. Additional details on this method can be found in Drennan et al. (2007). Neutral 10-m specific humidity $q_{10N}$ was estimated using a logarithmic profile to extrapolate the flight-level measurements to 10 m. The moisture exchange coefficient, or Dalton number ($C_{E10N}$, referred to hereafter as $C_E$), for each flux run was computed directly from the humidity flux $U_{10N}$, $q_0$, and $q_{10N}$. Details and justification of the above discussion can be found in French et al. (2007) and Drennan et al. (2007). Of course, in an environment where individual wave heights can exceed 20 m, the meaning of 10-m bulk coefficients should be questioned. We consider them to be useful as reference values, with 10 m being the lowest level for many atmospheric models.

When CBLAST $C_D$ and $C_E$ results are compared with other studies (Figs. 5 and 6), one can see that they represent a 32% and 61% increase, respectively, of the wind speed range of prior observations. It is apparent that the CBLAST high-wind $C_D$ values represent a systematic departure from prior estimates. Several surprising results emerged from these measurements. Primarily, CBLAST $C_D$ measurements

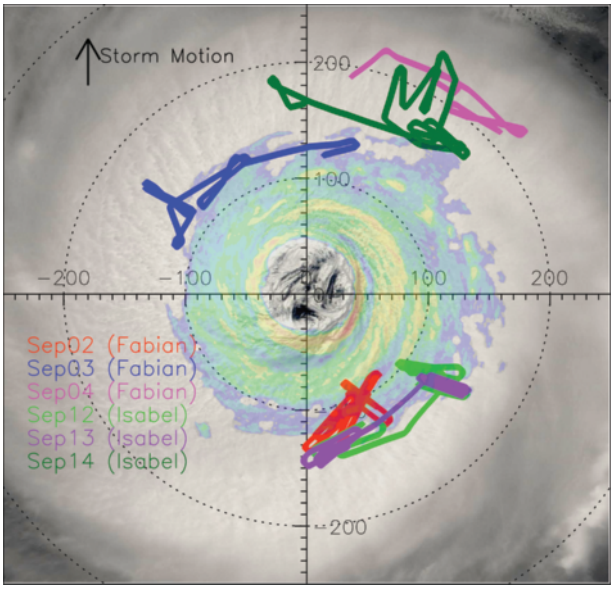


**Fig. 4. CBLAST stepped-descent flight patterns flown in Hurricanes Fabian and Isabel in 2003, plotted in storm-relative coordinates, with the storm motion indicated by the arrow (up). Circles are shown at 100-km intervals. Flight tracks are superimposed on NASA MODIS visual image of Hurricane Isabel at 1445 UTC 14 Sep 2003. In addition, a WP-3D LF airborne radar image from NOAA 43 of Isabel at 1642 UTC is overlaid indicating typical eyewall and rainband structure. MODIS image courtesy of MODIS Rapid Response Project at NASA GSFC.**

become nearly invariant with wind speed above a 23 m $s^{-1}$ threshold (Fig. 5). This is a full 10–12 m $s^{-1}$ less than the hurricane-force threshold of 33 m $s^{-1}$ obtained using GPS dropsonde measurements by Powell et al. (2003) and laboratory tank measurements by Donelan et al. (2004).

CBLAST $C_D$ measurements (Fig. 5) agree with previous open-ocean, gale-force wind measurements in the range of 17–22 m $s^{-1}$ for fully developed seas in the North Pacific at Ocean Weather Ship Papa (Large and Pond 1981), in the North Atlantic at Sable Island (Smith 1980), and in the Southern Oceans from a research vessel (Yelland et al. 1998). Values are lower than $C_D$ observations in fetch-limited wave conditions during HEXOS in the North Sea (Smith et al. 1992) for COARE 3.0 conditions (Fairall et al. 2003) and for CBLAST-Low (Edson et al. 2007). Estimates of $C_D$ show little dependence on the quadrant of the storm in which the measurements were obtained. However, it should be noted that the natural variability in the data provide less-than-overwhelming confidence of this result. The value of $C_D$ differs little between regions of young, growing waves in the right-rear quadrant in a swell-following environment and regions in the right-front and left-front quadrants where the local sea was older, less steep, and higher, with swell at increasing crossing angles with respect to the wind of up to 90° (Wright et al. 2001), a result that is discussed further in the following subsection. Another new finding suggests that moisture flux measurements are relatively constant with height within the hurricane boundary layer. Finally, we find that estimates of $C_E$ above 20 m $s^{-1}$ are in good agreement with the results from HEXOS (DeCosmo et al. 1996; modified as per Fairall et al. 2003) and COARE 3.0 (Fairall et al. 2003) extrapolated from 19 m $s^{-1}$ through our range of measurements (Fig. 6). This suggests that $C_E$ is constant with wind speed up to hurricane-force winds of 33 m $s^{-1}$.

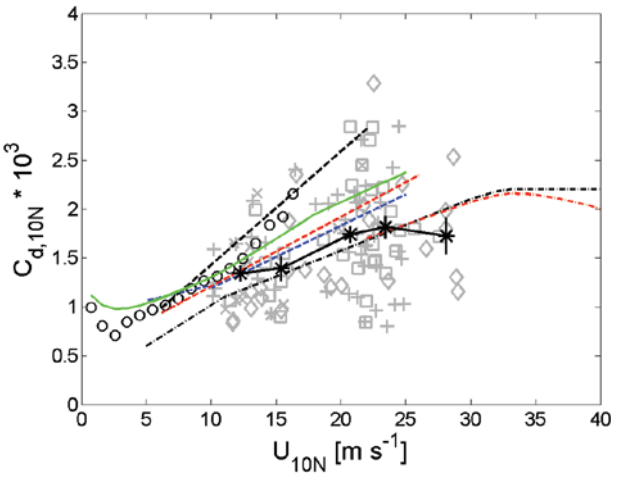


**Fig. 5. Drag coefficient estimates derived from CBLAST stepped-descent flight legs in Hurricanes Edouard, Isadore, and Lili (2002), Fabian and Isabel (2003), and Frances and Jeanne (2004). The asterisks represent average values in 2.5 m $s^{-1}$ bins, and the bars show 95% confidence intervals. The squares are from flight legs in the right-front quadrant of the storms, the plus signs from the right-rear quadrant, and the diamonds from the left-front quadrant. The black dash–dot line represents the values from Donelan et al. (2004); the red dash–dot line from Powell et al. (2003); blue dashed line from an average of Smith (1980) and Large and Pond (1981); the red dashed line from Yelland et al. (1998); black dashed line from HEXOS (Smith et al. 1992), and the gray circles from CBLAST-Low (Edson et al. 2007).**

It is obvious that while CBLAST extended the wind speed range of prior $C_D$ and $C_E$ observations, a further increase of the wind speed range is required to validate flux estimates in hurricane-force wind conditions, where physical processes may depart significantly from tropical storm wind conditions as the importance of sea spray and other poorly understood phenomena, such as "roll vortex" features, may in-

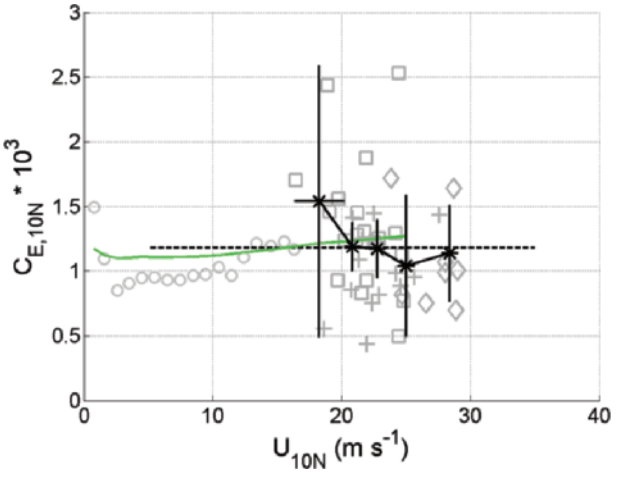


**Fig. 6. Moisture exchange coefficient (Dalton number) estimates derived from CBLAST stepped-descent flight legs in Hurricanes Fabian and Isabel (2003). The asterisks represent average values in 2.5 m $s^{-1}$ bins, and the bars show 95% confidence limits. The squares are from flight legs in the right-front quadrant of the storms, plus signs from the right-rear quadrant, and diamonds from the left-front quadrant. The black dashed line represents the HEXOS line (DeCosmo et al. 1996), modified as per Fairall et al. (2003) and extended to 36 m $s^{-1}$. The green solid line is the COARE 3.0 curve (Fairall et al. 2003), and the gray circles are from CBLAST-Low (Edson et al. 2007).**

crease dramatically. Budget and sea-spray studies are underway to estimate $C_D$ and $C_E$ for hurricane-force conditions by K. A. Emanuel (2006, personal communication) using the CBLAST rapid-deployment eyewall dropsondes in Hurricanes Fabian and Isabel and by C. W. Fairall (2006, personal communication) using laboratory measurements.

Emanuel (1986, 1995) has shown that the ratio of $C_E/C_D$ is an important parameter in estimating hurricane potential intensity. The new $C_D$ and $C_E$ observations, along with the new highly reliable SFMR surface wind measurements (Uhlhorn and Black 2003; UHL06), show $C_E/C_D$ values to average near 0.7 for tropical storm conditions, which is slightly below the Emanuel (1995) threshold for hurricane development of 0.75 (Fig. 7). The $C_E/C_D$ ratio estimates from the budget methodology by K. A. Emanuel (2006, personal communication) for axisymmetric mean surface winds of 50 m $s^{-1}$ in Isabel suggest that the ratio may increase significantly above our values for intense hurricane conditions. On the other hand, Andreas and Emanuel (2001) have suggested that the role of spray may act to simultaneously increase $C_D$ and $C_E$, leaving the ratio nearly equal to our values at high winds. This would require another explanation for how intense hurricanes develop and are maintained. The implications of $C_E/C_D$ ~ 0.7 for intense storms have been investigated by Montgomery et al. (2006) and Bell and Montgomery (2007, submitted to *Mon. Wea. Rev.*), which indicate that "superintense" conditions leading to sustained category 4 and 5 conditions, such as are observed in Isabel, are a result of the strong air–sea interaction inward from the hurricane eyewall leading to augmented horizontal entropy transport via enhanced frictional inflow and eyewall mesovortices. They suggested that this mechanism was a key reason why Isabel maintained category 5 status for 3 days.

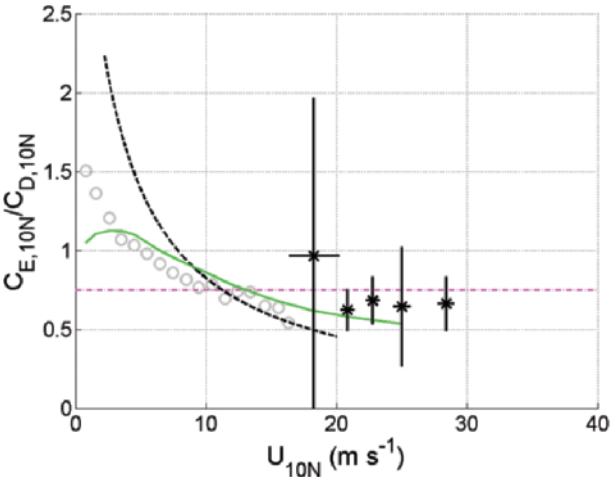


**FIG. 7. Ratio of $C_E/C_D$ derived from CBLAST measurements. The asterisks represent average values in 2.5 m $s^{-1}$ bins, and the bars show 95% confidence limits. The black dashed curve is the mean ratio from HEXOS (DeCosmo et al. 1996; modified as per Fairall et al. 2003; Smith et al. 1992). The solid green line is the ratio values from COARE 3.0 (Fairall et al. 2003). The gray circles are from CBLAST-Low (Edson et al. 2007). The dash–dot horizontal magenta line is the 0.75 threshold for TC development proposed by Emanuel (1995).**

*Surface wave observations.* The SRA on one of the P3 aircraft recorded huge datasets of wave images and 2D wave spectra in all quadrants of CBLAST storms in Fabian in 2003 and throughout the CBLAST storms in 2004. A wave image typical of this dataset (Fig. 8) from the front quadrant of Hurricane Fabian near 500-m flight altitude illustrates the predominant 300-m swell. Superimposed on the swell is the local sea with wavelengths of about 80–100 m crossing at a 90° angle. This is typical of conditions depicted in sector III of Fig. 9, which illustrate three sectors of distinctly different 2D wave spectra in Hurricane Bonnie (1998), discussed by Wright et al. (2001). The spectra in sector I tend to be short wavelength and unimodal.. The spectra in sector II tend to transition to bimodal, then trimodal with two swell peaks plus the local sea, then back to bimodal, with the swell following within 30° of the local sea. The spectra in sector III tend to transition from bimodal to unimodal depending on whether the local sea is resolved. The swell tends to propagate at about a 90° angle to the local sea in this region.

An additional illustration of the behavior of the swell relative to the local sea as a function of azimuth is shown in Fig. 10, from SRA measurements throughout Hurricane Ivan (2004). Figure 10 shows an HRD H*WIND surface wind analysis (Powell and Houston 1996; Powell et al. 1998; Powell and Houston 1998), based primarily on SFMR surface wind data, for Hurricane Ivan on 14 September 2004 when Ivan was moving northwest. Twelve SRA spectra about 80 km from the eye are shown in Fig. 10. In the right-front quadrant (the sector II–III boundary), the wave field is unimodal with 350-m wavelength and 11.4-m wave height. Directly to the right of the track the wavelength shortens to about 260 m and the spectrum broadens and becomes bimodal. In the right-rear quadrant the wave height decreases and the spectrum becomes trimodal. In the rear quadrant of Ivan, as was the case with Bonnie (Fig. 9), the wave height and length reach minimum values of 5.6 and 190 m, which are about half their values in the right-forward quadrant. This

suggests that the waves are young, steep, and short in the right-rear quadrant, and older, flatter, and longer in the right-front and left-front quadrants. To the left rear and left front of the eye, the wind and waves are at about right angles to each other.

The expectation was that the exchange coefficients would exhibit a variability that depended on the characteristics of the 2D wave spectrum. This has turned out to not be the case, as one can see by comparing Figs. 5 and 6 with Fig. 10. What this says, and what emerges as the second major conclusion for CBLAST-Hurricane measurements, is that surface fluxes and exchange coefficients (Figs. 5–6) appear not to be a function of the variation in the relationship between the long-wavelength swell and the shorter-wavelength local sea, at least between tropical storm– and hurricane-force wind radii.

*Evidence for secondary boundary layer circulations.* Strong evidence was found for the existence of roll vortex secondary boundary layer circulations in hurricanes. Complementing the CBLAST flights in 2002–04 were a number of RADARSAT and ENVISAT SAR passes (see Fig. 11, top) over the storms, which all showed streaks in the radar backscatter with wavelengths on the order of 800–1,000 m. These were most prominent in the front semicircle of the storm. Spectral analysis of these images over 5 km$^2$ ocean cells was able to retrieve a direction that was nearly equal to the wind direction, as well as a mean wavelength (Katsaros et al. 2002). Figure 11 (bottom) illustrates a histogram averaged over six such 2D spectra (6 km$^2$) that shows a peak near 900 m. This value is close to that determined from ground-based WSR-88D radar observations in landfalling

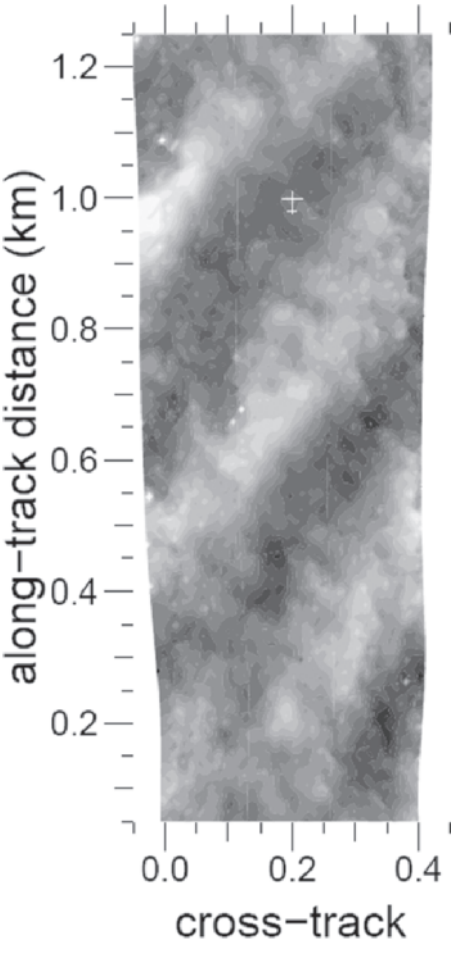


**Fig. 8. Swath of wave elevations from SRA from 500-m flight altitude during Fabian, in 2003. Scale of aircraft is shown at 1-km along-track, 0.2-km cross-track position.**

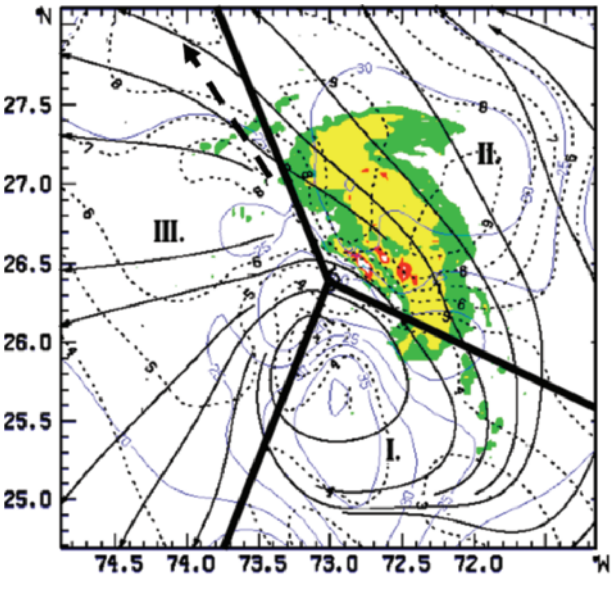


**Fig. 9. Analysis of SRA primary swell direction of propagation (solid black "streamlines"), wave height in meters (dashed black contours) and wave steepness × 10$^{-3}$ (thin solid blue contours) for Hurricane Bonnie at 2052 UTC 24 Aug 1998. Measurements are made at an aircraft altitude of 1550 m. Asymmetric convective radar reflectivity contours in dBZ are 28 (green), 35 (yellow), 41 (red), and 48 (white). Storm is divided into three sectors according to wave-directional characteristics: I: Unimodal, short-wavelength (~150–200 m) waves moving with the wind; II: bimodal or trimodal spectra shifting to longer wavelengths (~200–300 m), outward relative to dominant waves moving outward by up to 45°, relative to the wind direction; and III: unimodal spectra with peak long-wavelength waves (~300–350 m) moving outward relative to the wind by 60°–90°. Direction of storm motion is indicated by the bold dashed arrow.**

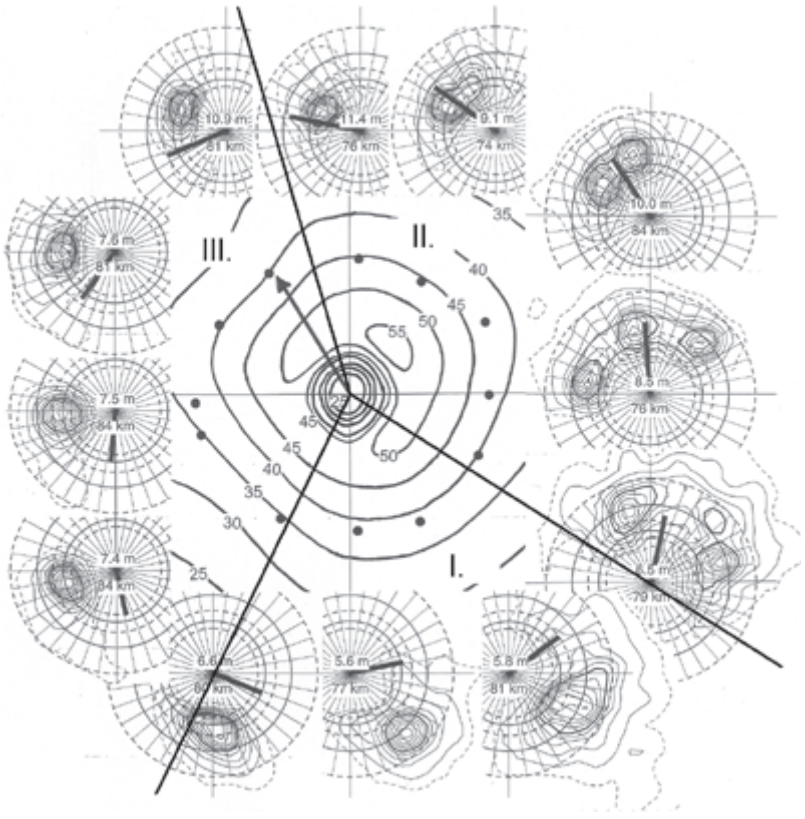


**Fig. 10. The center of the figure shows wind speed contours (m $s^{-1}$) from the HRD H*WIND surface wind analysis, based mainly on SFMR surface wind speed measurements in Hurricane Ivan at 2230 UTC 14 Sep 2004 for a 2° latitude and longitude box centered on the eye. Arrow at the center indicates Ivan's direction of motion (330°). Solid black lines separate three sectors (I.–III.) defining distinctly different wave spectra. The storm-relative locations of twelve 2D surface wave spectra measured by the SRA are indicated by the black dots. The spectra have nine solid contours linearly spaced between the 10% and 90% levels relative to the peak spectral density. The dashed contour is at the 5% level. The outer solid circle indicates a 200-m wavelength and the inner circle indicates a 300-m wavelength. The dashed circles indicate wavelengths at 150, 250, and 350 m (from outer to inner). The thick line at the center of each spectrum points in the downwind direction, with its length proportional to the surface wind speed. The upper number at the center of each spectrum is the significant wave height and the lower number is the distance from the center of the eye. The average radial distance for the 12 spectral locations is 80 km. The SRA data, which produced the spectra, were collected between 2030 UTC 14 September and 0330 UTC 15 September.**

hurricanes (Morrison et al. 2005). Their results are supported by more recent higher-resolution portable Doppler radar observations in landfalling hurricanes (Losorlo and Schroeder 2006a,b) and by DOW high-resolution portable Doppler radar observations in Hurricane Fran (Wurman and Winslow 1998), and more recently in Hurricane Rita (Wurman et al. 2006). With these studies, the range of wavelengths of these linear features are well documented over land in landfalling hurricanes. Now, RADARSAT and ENVISAT SAR observations suggest they are also endemic to the hurricane wind field over the ocean.

To further emphasize the possible layer manifestation of these linear features, the along-wind component of the velocity cospectrum was computed from gust-probe data in Hurricane Isidore (2002) along a 75-km leg flown at 300 m, near the middle of the hurricane well-mixed boundary layer with a depth of 500 m (deduced from the depth of constant potential temperature layers measured by dropsondes). The first part of the leg was in the radial direction toward the eye and showed a significant peak in the cospectrum near 900 m (Fig. 12), in close agreement with the scales from the SAR histogram (Fig. 11, bottom). This peak disappeared when the aircraft turned and flew along wind. The significance of these observations is that these linear features, and their possible major effect on air–sea fluxes [as suggested by Morrison et al. (2005) and Foster (2005)], are not currently modeled in any major hurricane-coupled modeling effort, and may be an important factor in the prediction of hurricane intensity change. This leads to the third major CBLAST finding to date, that is, that secondary boundary layer circulations, which while not a major thrust of the original CBLAST plan, are a significant factor in the hurricane boundary layer flow field and are a likewise significant factor in air–sea fluxes.

**KEY RESULTS FROM THE AIR-DEPLOYED OCEANOGRAPHIC SENSOR COMPONENT OF CBLAST-HURRICANE.** The 52 buoys and floats deployed into Hurricane Frances in 2004 yielded a wealth of information on ocean structure and structure changes induced by the hurricane within and below the ocean mixed layer: the first-ever 4D ocean structure observations beneath a hurricane.

Detailed measurements of the ocean and air–sea interface beneath hurricanes were made using several varieties of autonomous floats and drifters that were air deployed ahead of the storm. The technology for these devices has matured rapidly in recent years so that they are now deployed in large numbers as part of the developing system for the IOOS. For CBLAST, air-deployment systems were developed for existing platforms and they were equipped with new sensors to measure properties of the air–sea interface. The goal of these investigations was to understand the properties of the air–sea interface and upper ocean at wind speeds greater than 30 m $s^{-1}$ in order to determine the associated air–sea fluxes and the effect of these on hurricane intensification.

The region of high winds beneath a hurricane is quite small: a few hundred kilometers in diameter for the largest storms, and much less for a typical storm. Accordingly, the probability of measuring high winds from an array of instruments prepositioned in "hurricane alley" is small. As with meteorological studies of hurricanes, a viable sampling plan must rely on real-time measurements of storm position, reliable forecasts of future storm tracks, and the ability of the aircraft to deploy sensors in or near an active storm based on this information. Accordingly, close cooperation was essential between the NHC, which supplied the storm forecasts, the scientific team, who adapted the sampling array to these changing conditions, and the AFRC 53rd WRS, who deployed the instruments. Equally important was the use of UNOLS ships to recover the floats after the hurricane had passed.

The five varieties of oceanographic instruments used in CBLAST-Hurricane can be divided into the following two categories: *drifters* and *floats*. Details of each instrument type are shown in Table 3. Figure 13 shows drawings of each instrument and a schematic of their operation in Hurricane Frances (2004).

Drifters aim to follow the ocean current at 15-m depth while measuring both near-surface atmospheric and upper-ocean properties. A small surface float supports a much larger drogue centered at 15-m depth. The large drogue causes the drifter to nearly follow the horizontal water motion at approximately 15 m. A transmitter in the surface drifter sends data to the *Argos* satellite system. The same signals are used to track the drifter. The standard drifter measurements are position and near-surface temperature. The CBLAST drifters carried additional sensors. Minimet drifters are also designed to estimate wind speed using the sound level at 8 kHz (Nystuen and Selsor 1997) and wind direction using a vane on the surface float. Evaluation of the accuracy of this approach at hurricane wind speeds is

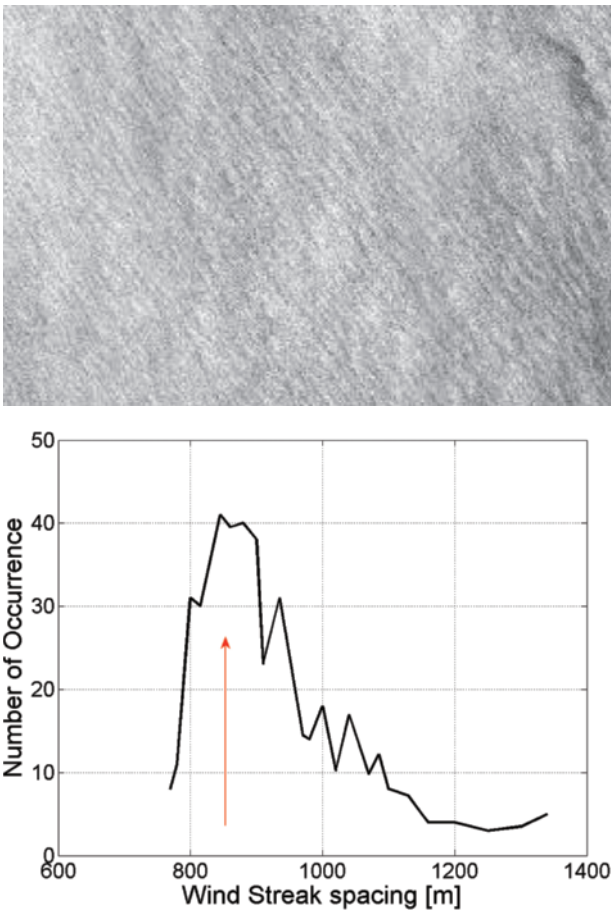


**Fig. 11. (top) RADARSAT SAR image from right-front quadrant of Hurricane Fran, similar to that obtained for Hurricane Isidore (2002). The horizontal scale is 200 km. (bottom) Histogram of wind streak wavelengths from analyzed RADARSAT image of Hurricane Isidore (23 Sep 2002). Arrow indicates peak in aircraft-derived spectrum in Fig. 12. RADARSAT image courtesy of Canadian Space Agency.**

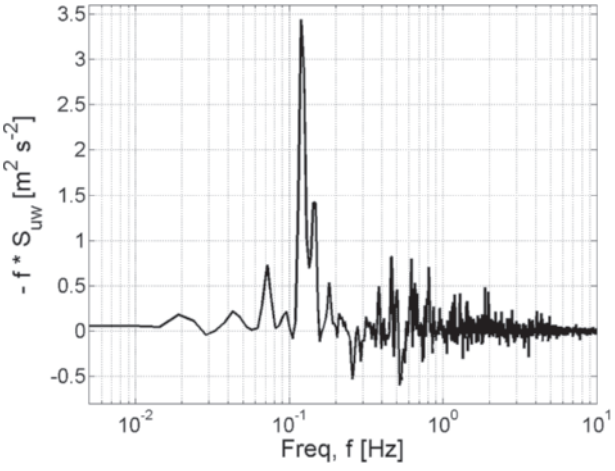


**Fig. 12. Cospectrum of vertical momentum flux (–*u*'*w*') along a 120-m-altitude radial flight leg into Hurricane Isidore (22 Sep 2002). The true air speed is 110 m $s^{-1}$.**

| Table 3. Oceanographic platforms deployed in CBLAST-Hurricane. | | | | | |
|---|---|---|---|---|---|
| | **MiniMet** | **ADOS** | **EM-APEX** | **Lagrangian** | **SOLO** |
| **Type** | Drifter | Drifter | Float | Float | Float |
| **Measurements** | SST, air pressure, wind speed, wind direction, position, | SST, air pressure, wind speed, wind direction, temperature 0–120 m, position | Temperature, salinity, pressure, velocity, position, | Temperature, salinity, pressure, gas tension, oxygen, position | Temperature, salinity, pressure, oxygen, sound 0–50 kHz, wave height, position |
| **Satellite** | Argos | Argos | Iridium | Iridium | Orbcomm |
| 2003 deployed | 16 | | | 4 | 2 |
| 2004 deployed | 30 | 8 | 3 | 2 | 9 |

still under way. ADOS drifters additionally measure the temperature profile to 100-m depth.

The three varieties of floats are shown in Fig. 13. All floats operate by mechanically changing their volume, and thus their density, in order to control their depth. By making themselves light, they can profile to the surface, thereby extending an antenna out of the water, enabling them to obtain a GPS fix and relay data to and receive instructions from their shore-based operators. The EM-APEX floats (Fig. 13, green lines) operated as profilers, continuously cycling while measuring temperature, salinity, and velocity. Profiles extended from the surface to 200 m with profiles to 500 m every half inertial period. During the storm, the top of the profiles terminated at 50 m. The Lagrangian floats (D'Asaro 2003) profiled only before and after the storm (Fig. 13, black line). During the storm, they remained neutrally buoyant, following the three-dimensional motion of water parcels in the highly turbulent upper boundary layer. They measured temperature, salinity, and gas concentration. The SOLO floats profiled temperature, salinity, and oxygen from the surface to approximately 200 m (Fig. 13, blue line) while hovering at about 40 m for a period of time during each dive interval to remotely measure surface waves and the depth of the bubble layer created by surface wave breaking, using a compact sonar and 0–50–kHz ambient sound with a passive hydrophone. The floats were programmed to repeat its dive interval every 4 hours.

Initial deployments were made in Hurricane Isidore in 2002 and Fabian in 2003. The more extensive 2004 deployments ahead of Hurricane Frances will be described here. The array of floats and drifters (Fig. 14) was deployed from 2000 to 2300 UTC 31 August 2004 based on the 0300 UTC 31 August forecast for the 1800 UTC 1 September storm position. The storm track passed just north of the shallow banks and islands north of Hispaniola. The array was therefore placed over deep water north of the storm track. The forecast proved to be extremely accurate, so that array elements passed under both the eye and maximum winds (60 m $s^{-1}$) of the storm.

The Hurricane Frances deployments clearly demonstrated the success of this new approach to measurement in hurricanes. The instruments were accurately targeted into the category 4 hurricane. All of the varieties of drifters and floats survived and worked successfully in this environment, with only minimal

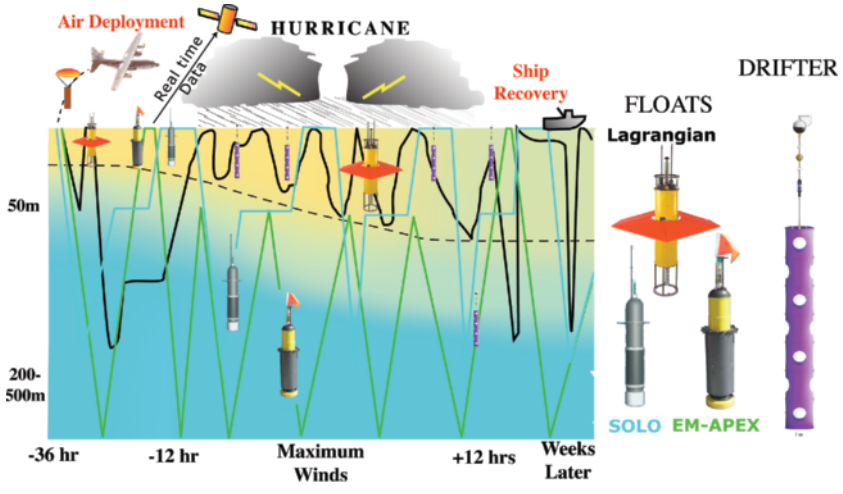


**Fig. 13. Drawings of the three varieties of floats and a surface drifter as deployed into Hurricane Frances. Schematic depicts operations in Hurricane Frances (2004).**

losses. Data were transmitted from the high-wind region of the hurricane in near–real time.

The buoys and floats revealed a warm anticyclonic eddy directly in the path of Frances, which was flanked by cooler cyclonic features. Sea surface height anomaly maps from satellite altimetry for the North Atlantic (see Atlantic map online at www.aoml.noaa.gov/phod/cyclone/data, iwave.rsmas.miami.edu/heat/, or www7320.nrlssc.navy.mil/hhc/), such as the area along 30°N east of northern Florida, sometimes referred to as the "subtropical convergence zone," indicates the presence of an eddy-rich ocean in the vicinity of the storm track.

Parameterization of the air–sea fluxes that drive hurricanes depends on an understanding of the air–sea interface at high wind speeds. Figure 15 shows the ability of the floats to make detailed measurements of surface waves and near-surface bubble clouds across the hurricane. The time-varying height of the sea surface was measured by the SOLO floats using an upward-looking sonar that compensated for the measured float depth. High-frequency fluctuations in sea height yield measurements of the surface waves. Maximum significant wave height exceeded 10 m. Intense breaking of these large waves injects bubbles into the ocean. The resulting near-surface bubble layer plays a key role in gas flux across the air–sea interface, and as well has an important dynamical effect by changing the bulk density of the near-surface layer. Bubbles are very efficient sound scatterers, so that the thickness of the near-surface bubble layer can be measured by the upward-looking sonar. Its thickness increases approximately as wind speed cubed, reaching a maximum thickness of over 10 m. These results are confirmed by Lagrangian float measurements of conductivity, which decreases in the upper 10 m due to bubbles.

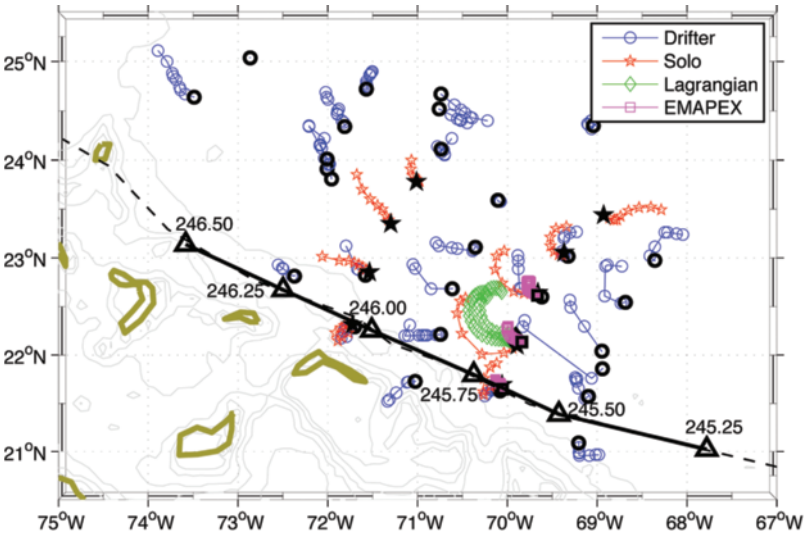


**Fig. 14. Hurricane Frances (2004) float and drifter array. Heavy line shows storm track, labeled by Julian day (JD 245.00 = 0000 UTC 1 September). Colors indicate type of instrument. Instrument tracks are plotted from deployment on JD 244 (31 August) to JD 246.5 (1200 UTC 2 September). Deployment position is indicated by black symbol.**

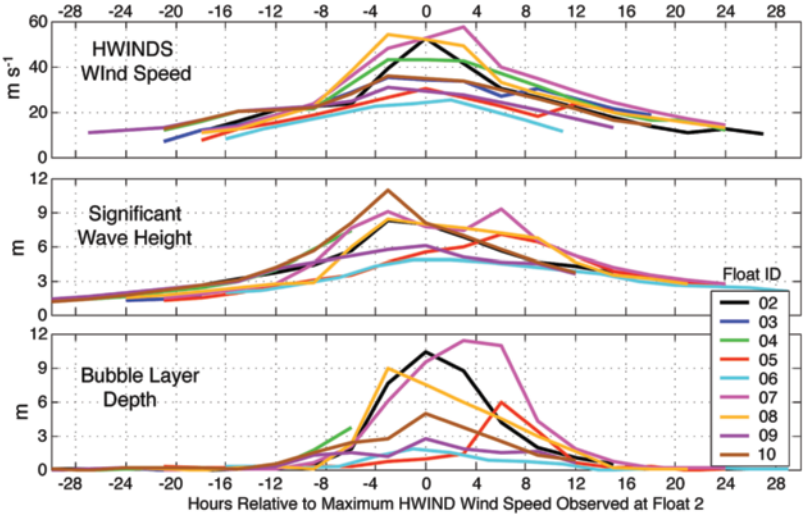


**Fig. 15. Significant surface wave height and bubble cloud depth measured by the nine SOLO floats and wind speed at the float location from H*WIND analysis. Time axis is hours from time of maximum wind at each float.**

Hurricanes draw their energy from the warm ocean waters. However, ocean mixing beneath a hurricane can significantly reduce sea surface temperatures from the prestorm values. Figure 16 shows the evolution of upper-ocean potential density under the strongest winds of Hurricane Frances. It combines the vertical temperature profiles from an EM-APEX float with the nearby temperature measurements from the two Lagrangian floats. The EM-APEX floats also showed the evolution of the currents in the

upper ocean (Sanford et al. 2005). Figure 16 shows rapid deepening of the mixed layer and associated high shear across the thermocline. The strong wind and wave forcing directly generates turbulence in the upper 20–40 m of the ocean. The Lagrangian floats are advected by the large-eddy velocities of this turbulence, repeatedly cycling across the turbulent layer and thereby tracing its depth and intensity (red and blue lines, respectively). Turbulent velocities are 0.1 m $s^{-1}$ rms at the height of the storm, with the strongest downward vertical velocities reaching 0.3 m $s^{-1}$. The turbulent layer extends to 50 m at the height of the storm. However, the changes in temperature indicate that mixing extends to 120 m (magenta line). Measurements of shear by the EM-APEX floats show (Fig. 17) a nearly critical Richardson number down to 120 m, indicating a key role for shear instability in this deeper mixing. The one-dimensional heat budget requires even deeper mixing as shown by the yellow-dashed line (Fig. 16, bottom panel). A more detailed analysis indicates that horizontal heat fluxes become important as the magenta and yellow-dashed lines diverge, indicating a transition of the boundary layer heat budget from vertical to three-dimensional.

The net effect of this strong ocean mixing is to cool the ocean surface, potentially reducing the enthalpy flux to the hurricane. The combined data from the floats and drifters are used to map the amount of cooling in Fig. 18. Cooling is most intense to the right of the storm center, with a cold wake spreading outward behind this region. The leading edge of this wake forms an SST front approximately 50 km wide, which moves with the storm. The eye of the storm is at the edge of this front, so that cooling at the eye is only about 0.5°C compared to the maximum of 3.2°C in a crescent-shaped pattern in the storm's right-rear quadrant, similar to that proposed by Black et al. (1988). SST gradients up to 2°C exist across the inner 50 km of the storm, with a temperature range of about 27.5°–30°C. These data suggest that rather than specifying the SST at the hurricane inner core, it may be more useful to think in terms of the location of the SST front that exists beneath the core. Small changes in the location of this front relative to the core may have large effects on the enthalpy flux driving the storm.

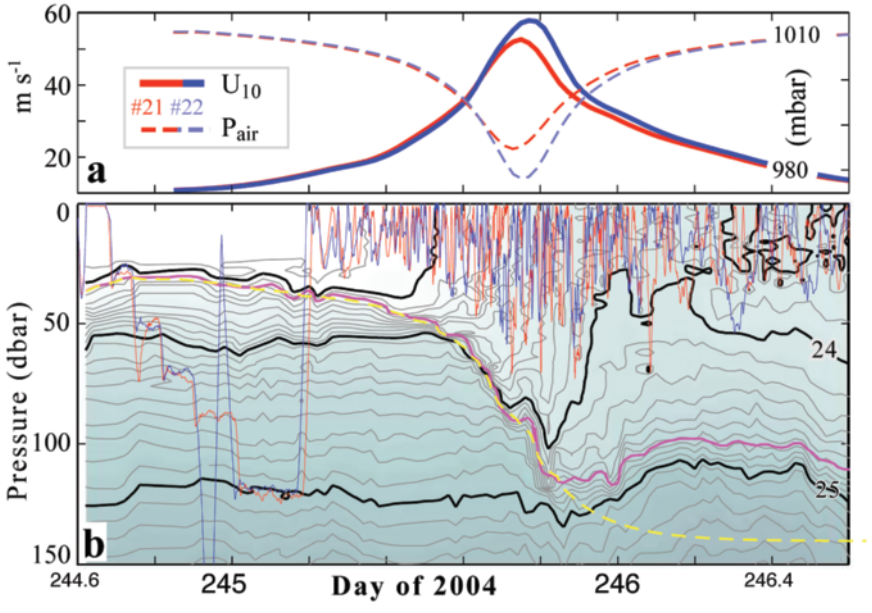


**Fig. 16. Evolution of the density structure of the upper ocean near the radius of maximum winds of Hurricane Frances. (a) Wind speed and atmospheric pressure from HRD H*WIND analysis at the two Lagrangian floats. (b) Potential density contours (kg $m^{-3}$; in black), trajectories of Lagrangian floats (red and blue), measured depth of the mixed layer (magenta), and estimated depth of the mixed layer from a vertical heat budget (yellow, dashed).**

**SUMMARY AND CONCLUSIONS.** The CBLAST-Hurricane program has yielded an unprecedented dataset for exploring the coupled atmosphere and ocean boundary layers during an active hurricane. Key results from the analysis effort to date have increased the range of air–sea flux measurements significantly, which have allowed drag and enthalpy exchange coefficients to be estimated in wind speeds to nearly hurricane force. The drag coefficients ($C_D$s) estimated from this work suggest a leveling off with wind speed near 22–23 m $s^{-1}$, which is a considerably lower threshold than the 33 m $s^{-1}$ value of Powell et al. (2003) and Donelan et al. (2004). This results in extrapolated $C_D$s for hurricane conditions above 33 m $s^{-1}$ of under 0.002, slightly lower than the results of Powell et al. (2003) and Donelan et al. (2004) for the 30–40 m $s^{-1}$ wind speed interval, which are approximately 0.0022. The Dalton number is constant with wind speed up to hurricane force with a value of 0.00118, in close agreement with modified HEXOS and COARE 3.0 estimates. This results in $C_E/C_D$ ratio of approximately 0.7, which is somewhat less than the Emanuel threshold

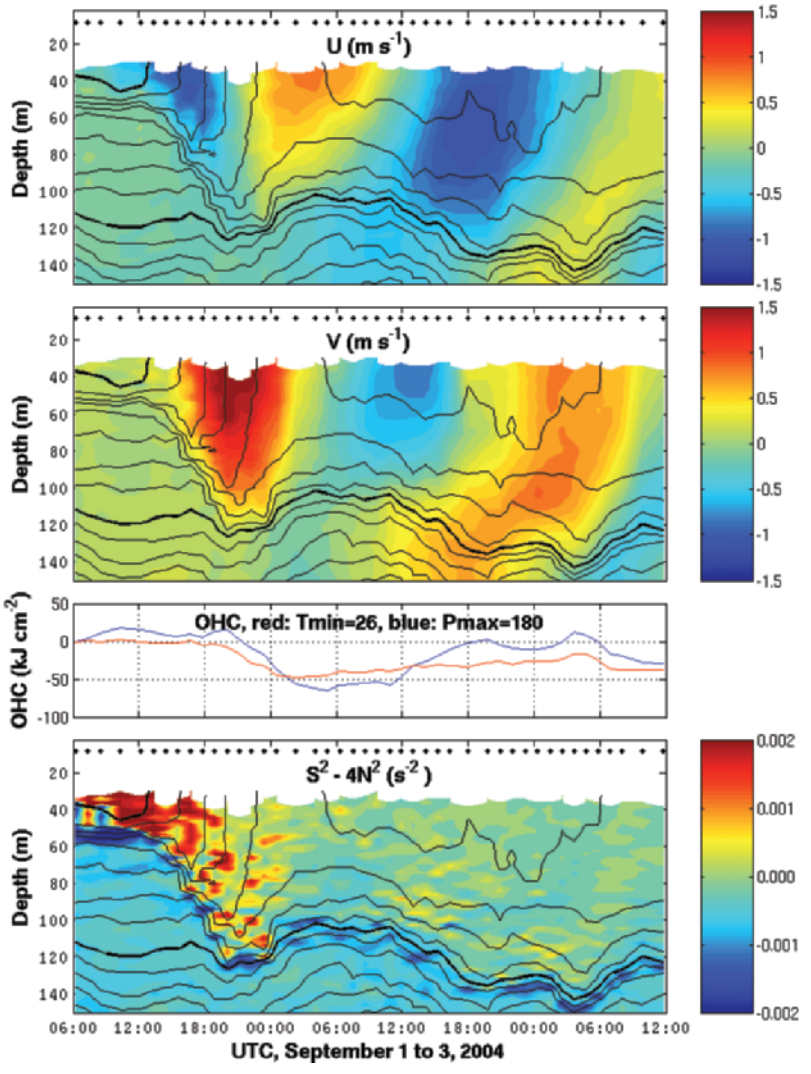


**FIG. 17. EM-APEX float 1633 located 50 km to the right of storm track in highest winds. The upper two panels are of east (*U*) and north (*V*) velocity components versus depth and time with the 29° and 25°C isotherms in bold with a contour interval of 0.5°C. The center of the storm passed at approximately 1700 UTC 1 September. OHC is shown for water warmer than 26°C and shallower than 180 m. The bottom panel is reduced shear, a stability parameter, with the temperature contours superimposed. This quantity is related to the Richardson number $Ri = N^2/S^2$, where *N* is the Brunt–Väisälä frequency and *S* is the vertical current shear. A necessary condition for shear instability is $N^2/S^2 < 1/4$. This instability criteria is rewritten as $S^2 - 4N^2 > 0$ to indicate where mixing is possible. The quantity $S^2 - 4N^2$ is contoured in the bottom panel with the green, yellow, and red colors indicating where the instability criteria is equaled or exceeded. The blue colors indicate stable conditions less than zero.**

of 0.75 for hurricane development. Directional wave measurements made from the aircraft show distinctive characteristic as a function of storm-relative quadrant. Spectra range from trimodal in the right-rear quadrant to bimodal in the right-front to unimodal in the left-front quadrant. The exchange coefficients appear independent of these wave spectral characteristics to within observational uncertainty. Boundary layer linear features (possible secondary circulations or "roll" vortices) appear to characterize the boundary layer throughout the hurricane with their role in flux estimation yet to be determined.

The drifter and buoy deployments in Hurricanes Fabian (2003) and Frances (2004) were unqualified successes, yielding first-time-ever observations of the four-dimensional evolution of the subsurface ocean structure concurrent with airborne atmospheric

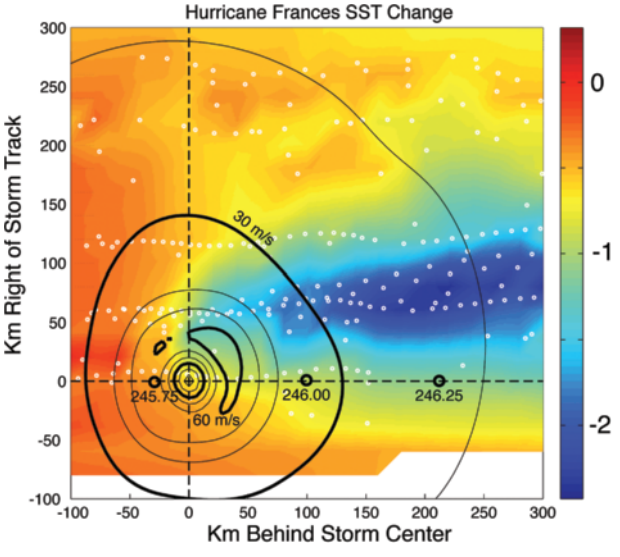


**FIG. 18. SST decreases (°C) beneath hurricane Frances (2003) in storm-centered coordinate system. White dots show storm-relative locations of float and drifter data. Storm motion is to the left. Colors show mapped SST change from prestorm value. Contours show wind speed (m $s^{-1}$) from H*WIND analysis. Storm positions are in increments of one-quarter JD, or 6 h, where JD 245 is 1 September.**

boundary layer observations. The development of the cold wake behind Frances, showing a crescent-shaped pattern of cooling in the near-storm environment, was well observed with maximum cooling of 3.2°C. Shear at the base of the ocean mixed layer was found to develop quickly beneath the hurricane and meet the Richardson number criteria of 1/4 for onset of turbulent mixing.

The analyses of this immense dataset is ongoing. Incorporation into research and operational coupled models is just beginning. The outlook for major impacts on these modeling efforts is optimistic.

**FUTURE PLANS FOR CBLAST-HURRICANE.** The analysis of CBLAST-Hurricane datasets has just begun. Continued support for analysis efforts has been provided by ONR and by NOAA through the USWRP. Additional fundamental research will be ongoing in the years ahead for efforts, such as merging 2D wave spectra from the SRA and the 1D wave spectra from the SOLO floats to estimate the high-frequency portion of the wave spectrum and its impact on air–sea fluxes in hurricanes. The impact of sea spray on air–sea enthalpy and momentum fluxes is yet to be demonstrated in hurricane winds, especially for major hurricanes of category 3 and above. However, studies of foam whitecap coverage and wave-breaking percentage from high-speed digital camera images is ongoing in efforts to learn more about surface dissipation (Kleiss et al. 2004). Additional analysis is being carried out of the GPS sondes from the multisonde deployments in the hurricane eyewall for the purpose of estimating eyewall air–sea fluxes via budget calculations. From these, along with SFMR surface wind, SST, and specific humidity estimates, additional $C_D$ and $C_E$ values will be estimated for extreme winds in excess of 50 m $s^{-1}$. Work will continue on the diagnoses of boundary layer linear features (possible secondary circulations or "roll vortices") and their role in air–sea fluxes, including the variability by storm quadrant. Additional spectral analysis of BAT and LI-COR turbulence flux data from along- and cross-wind flight legs as well as analysis of IWRAP boundary layer and profiles (Esteban-Fernandez et al. 2004) will help to address the vertical structure of this phenomenon in the hurricane PBL. Continued synthesis of drift buoy, float, and satellite observations of ocean features in the path of Fabian and Frances will continue, including efforts to improve ocean-mixing parameterizations in hurricane conditions.

Efforts to estimate fluxes at the top of the hurricane boundary layer will begin. Using the suite of BAT and LI-COR turbulence instrumentation now available for both NOAA WP-3D aircraft, additional measurements will be sought over the coming years to fill gaps in the CBLAST datasets and to continue to focus on the parameterization with wind speed, wave conditions, and roll vortex effects. These observations will accompany new observations of sea-spray droplets from any low-level flights using the new suite of cloud microphysical spectrometer probes presently being improved on the P3 aircraft, opening the possibility of extending sea-spray studies.

The focus will also shift toward integrating existing and anticipated results on air–sea flux parameterization into high-resolution (1.7 km), coupled hurricane models such as that of Chen et al. (2007), as well as the new HWRF model, scheduled to become operational at the NOAA EMC during the 2007 hurricane season. EMC will also be examining the benefits of assimilating the profiling float data into their operational models to assess the value of deploying similar instruments in future storms to improve intensity predictions. Similarly, efforts are being made to integrate CBLAST results into the Navy NOGAPS and COAMPS models. Special efforts will begin to assess the impact of the new air–sea parameterization schemes on hurricane intensity.

We are at a unique point in history where airborne advanced technology is able to meet the requirements of the new generation of advanced coupled models for input and validation data in the hurricane, at the air–sea interface and in the ocean. Advances in hurricane computer modeling and observational technology are symbiotic. Continued investment in this effort now will produce large dividends at low risk for future improvements in hurricane intensity and track prediction.

**ACKNOWLEDGMENTS.** The authors and team of CBLAST investigators wish to thank the Office of Naval Research for supporting this work as a Departmental Research Initiative, Award Numbers N00014-01-F-009 (Black, Drennan, and French), N00014-01-1-0162 (Emanuel and Black), N00014-00-1-0894 (Terrill and Melville), N00014-00-1-0893 (D'Asaro), N00014-02-1-0401 (Niiler), and N00014-01-F-0052 (Walsh). The USWRP also supported Drennan with Grant Number NA17RJ1226. Walsh was also supported by the NASA Physical Oceanography Program. EM-APEX floats were developed with an ONR SBIR grant to Webb Research, Inc. We thank the NOAA OAR for P3 flight-hour and expendable dropsonde support for 3 years and to USWRP for CBLAST analysis support from 2005 to the present. Thanks are especially due to NOAA Deputy Assistant Administrator David Rogers for actively assisting in operational success of this experiment. We thank the NESDIS Ocean Winds project and lead PI

Paul Chang (also a CBLAST PI) for sharing flight-hour and dropsonde resources, without which the extensive effort over 3 years would have been impossible. We thank Frank Marks and the Hurricane Research Division staff for their infrastructure support for the NOAA aircraft field program effort, especially to Michael Black, Robert Rogers, and Chris Landsea who served as lead project scientists on many of the WP-3D flights. In particular, we thank Eric Uhlhorn of HRD, Alan Goldstein of AOC, and Ivan Popstefanija for ProSensing, Inc., for their support of the SFMR system during CBLAST flights. Special thanks are also due to James McFadden and the AOC for their dedicated effort over 4 years to work with CBLAST PI's to test and install their instruments and in many cases to redesign their instruments for hurricane flight conditions. We especially thank Terry Lynch and Sean McMillan and the electrical engineering staff for their constant efforts to keep the computer and experimental hardware operating in hostile conditions, and to Greg Bast and the aircraft flight engineer staff for their hard work to keep the aircraft in flight-ready status throughout the 3 years of active flights. Special thanks are due to Phil Hall, NOAA Corps, AOC, and ARL, for his extensive efforts to certify airworthiness for the BAT probe. We would also like to thank Phil Kennedy and the flight crews for the expert piloting and navigation of the aircraft. Thanks are especially due to Barry Damiano and Tom Shepard and the several flight directors who directed each CBLAST flight. Not one flight was cancelled and only one flight aborted due to mechanical problems. Special thanks are due to the 53rd WRS of the AFRS, for their extensive support of the buoy and float deployment effort, especially to Brigadier General Charles Ethredge and General Richard Moss who served as outgoing and incoming AFRC 403rd Wing Commanders during 2003–04. We would especially like to thank Chief Master Sergeant Robert E. Lee for supervising the airdrop training and bathroom renovations. Thanks to the many U.S. Air Force commands that participated in certifying the WC-130J, and individual platforms, to be deployed for airdrop capability. Finally, special thanks are due to ONR CBLAST Program Managers Simon Chang and Carl Friehe for actively helping to guide the program. Thanks are also extended to Scott Sandgathe, Steve Tracton, Linwood Vincent, Theresa Paluszkiewicz, and Ron Ferek for ONR management support. The assistance of Susanne Lehner, DLR Germany, and University of Miami in analysis of RADARSAT imagery is acknowledged.

## REFERENCES

Andreas, E. L., and K. A. Emanuel, 2001: Efffects of sea spray on tropical cyclone intensity. *J. Atmos. Sci.,* **58,** 3741–3751.

Black, P. G., R. I. Elsberry, and L. K. Shay, 1988: Airborne surveys of ocean current and temperature perturbations induced by hurricanes. *Adv. Underwater Technol. Ocean Sci. Eng.,* **16,** 51–58.

Chen, S. S., J. F. Price, W. Zhao, M. A. Donelan, E. J. Walsh, and H. L. Tolman, 2007: The CBLAST hurricane program and the next-generation fully coupled atmosphere–wave–ocean models for hurricane research and prediction. *Bull. Amer. Meteor. Soc.,* **88,** 311–317.

D'Asaro, E. A., 2003: Performance of autonomous Lagrangian floats. *J. Atmos. Oceanic Technol.,* **20,** 896–911.

DeCosmo, J., K. B. Katsaros, S. D. Smith, R. J. Anderson, W. A. Oost, K. Bumke, and H. Chadwick, 1996: Air-sea exchange of water vapor and sensible heat: The humidity exchange over the sea (HEXOS) results. *J. Geophys. Res.,* **101** (C5), 12 001–12 016.

DeMaria, M., M. Mainelli, L. K. Shay, J. A. Knaff, and J. Kaplan, 2005: Further improvements to the Statistical Hurricane Intensity Prediction Scheme (SHIPS). *Wea. Forecasting,* **20,** 531–543.

Donelan, M. A., 1990: Air–sea interaction. *The Sea,* B. LeMéhauté and D. Hanes, Eds., Ocean Engineering Science, Vol. 9, John Wiley and Sons, 239–292.

——, B. K. Haus, N. Reul, W. J. Plant, M. Stianssnie, H. C. Graber, O. B. Brown, and E. S. Saltzman, 2004: On the limiting aerodynamic roughness of the ocean in very strong winds. *Geophys. Res. Lett.,* **31,** L18306, doi:10.1029/2004GL019460.

Drennan, W. M., J. Zhang, J. R. French, C. McCormick, and P. G. Black, 2007: Turbulent fluxes in the hurricane boundary layer. Part II: Latent heat flux. *J. Atmos. Sci.,* in press.

Edson, J., and Coauthors, 2007: The Coupled Boundary Layers and Air–Sea Transfer Experiment in Low Winds. *Bull. Amer. Meteor. Soc.,* **88,** 341–356.

Emanuel, K. A., 1986: An air-sea interaction theory for tropical cyclones. Part I: Steady-state maintenance. *J. Atmos. Sci.,* **43,** 585–605.

——, 1995: Sensitivity of tropical cyclones to surface exchange coefficients and a revised steady-state model incorporating eye dynamics. *J. Atmos. Sci.,* **52,** 3969–3976.

Esteban-Fernandez, D., S. Frazier, J. Carswell, P. Chang, P. Black, and F. Marks, 2004: 3-D atmospheric boundary layer wind fields from Hurricanes Fabian and Isabel. Preprints, *26th Conf. on Hurricanes and Tropical Meteorology,* Miami Beach, FL, Amer. Meteor. Soc., CD-ROM, 1A.3.

Fairall, C. W., E. F. Bradley, J. E. Hare, A. A. Grachev, and J. B. Edson, 2003: Bulk parameterization of air–sea fluxes: Updates and verification for the COARE algorithm. *J. Climate,* **16,** 571–591.

Foster, R. C., 2005: Why rolls are prevalent in the hurricane boundary layer. *J. Atmos. Sci.,* **62,** 2647–2661.

French, J. R., W. M. Drennan, J. Zhang, and P. G. Black, 2007: Turbulent fluxes in the hurricane boundary layer. Part I: Momentum flux. *J. Atmos. Sci.,* in press.

Goldenberg, S. B., C. W. Landsea, A. M. Mestas-Nuñez, and W. M. Gray, 2001: The recent increase in Atlantic hurricane activity: Causes and implications. *Science,* **293,** 474–478.

Hebert, P. J., 1976: Atlantic hurricane season of 1975. *Mon. Wea. Rev.,* **104,** 453–475.

Katsaros, K. B., P. W. Vachon, W. T. Liu, and P. G. Black, 2002: Microwave remote sensing of tropical cyclones from space. *J. Oceanogr.,* **58,** 137–151.

Kleiss, J. M., W. K. Melville, J. R. Lasswell, P. Matusov, and E. Terrill, 2004: Breaking waves in hurricanes Isabel and Fabian. Preprints, *26th Conf. on Hurricanes and Tropical Meteorology,* Miami Beach, FL, Amer. Meteor. Soc., CD-ROM, 3A.1.

Large, W. G., and S. Pond, 1981: Open ocean momentum flux measurements in moderate to strong winds. *J. Phys. Oceanogr.,* **11,** 324–336.

Lorsolo, S., and J. R. Schroeder, 2006a: Small scale features observed in the boundary layer of Hurricanes Isabel (2003) and Frances (2004). *Proc. Air–Sea Interaction Conf.,* Atlanta, GA, Amer. Meteor. Soc., CD-ROM, 10.2.

——, and ——, 2006b: Tower and Doppler radar observations from the boundary layers of Hurricanes Isabel (2003) and Frances (2004). *Proc. 27th Conf. on Hurricanes and Tropical Meteorology,* Monterey, CA, Amer. Meteor. Soc., CD-ROM, 10.5.

Montgomery, M. T., M. M. Bell, S. Aberson, and M. Black, 2006: Hurricane Isabel (2003): New insights into the physics of intense storms. Part I: Mean vortex structure and maximum intensity estimate. *Bull. Amer. Meteor. Soc.,* **87,** 1335–1347.

Morrison, I., S. Businger, F. Marks, P. Dodge, and J. Businger, 2005: An observational case for the prevalence of roll vortices in the hurricane boundary layer. *J. Atmos. Sci.,* **62,** 2662–2673.

Moss, M. S., 1978: Low-level turbulence structure in the vicinity of a hurricane. *Mon. Wea. Rev.,* **106,** 841–849.

——, and F. J. Merceret, 1976: A note on several low-layer features of Hurricane Eloise (1975). *Mon. Wea. Rev.,* **104,** 967–971.

——, and ——, 1977: A comparison of velocity spectra from hot film anemometer and gust-probe measurements. *J. Appl. Meteor.,* **16,** 319–320.

Nystuen, J. A., and H. D. Selsor, 1997: Weather classification using passive acoustic drifters. *J. Atmos. Oceanic Technol.,* **14,** 656–666.

Powell, M. D., and S. H. Houston, 1996: Hurricane Andrew's landfall in south Florida. Part II: Surface wind fields and potential real-time applications. *Wea. Forecasting,* **11,** 329–349.

——, and ——, 1998: Surface wind fields of 1995 Hurricanes Erin, Opal, Luis, Marilyn, and Roxanne at landfall. *Mon. Wea. Rev.,* **126,** 1259–1273.

——, ——, L. R. Amat, and N. Morisseau-Leroy, 1998: The HRD real-time hurricane wind analysis system. *J. Wind Eng. Indust. Aerodyn.,* **77&78,** 53–64.

——, P. J. Vickery, and T. A. Reinhold, 2003: Reduced drag coefficient for high wind speeds in tropical cyclones. *Nature,* **422,** 279–283.

Sanford, T. B., J. H. Dunlap, J. A. Carlson, D. C. Webb, and J. B. Girton, 2005: Autonomous velocity and density profiler: EM-APEX. *Proc. Eighth Conf. on Current Measurement Technology,* Southampton, UK, IEEE/ OES, 152–156, IEEE Cat. No. 05CH37650, ISBN: 0-7803-8989-1.

Smith, S. D., 1980: Wind stress and heat flux over the ocean in gale force winds. *J. Phys. Oceanogr.,* **10,** 709–726.

——, and Coauthors, 1992: Sea surface wind stress and drag coefficients: The HEXOS results. *Bound.-Layer Meteor.,* **60,** 109–142.

Uhlhorn, E. W., and P. G. Black, 2003: Verification of remotely sensed sea surface winds in hurricanes. *J. Atmos. Oceanic Technol.,* **20,** 99–116.

Wright, C. W., E. J. Walsh, D. Vandemark, W. B. Krabill, S. H. Houston, M. D. Powell, P. G. Black, and F. D. Marks, 2001: Hurricane directional wave spectrum spatial variation in the open ocean. *J. Phys. Oceanogr.,* **31,** 2472–2488.

Wurman, J., and J. Winslow, 1998: Intense sub-kilometer scale boundary layer rolls observed in Hurricane Fran. *Science,* **280,** 555–557.

——, C. Alexander, P. Robinson, and F. Masters, 2006: Preliminary comparisons of DOW and in situ measurements in Hurricane Rita. *Proc. 27th Conf. on Hurricanes and Tropical Meteorology,* Monterey, CA, Amer. Meteor. Soc., CD-ROM, 10C.6.

Yelland, M. J., B. I. Moat, P. K. Taylor, R. W. Pascal, J. Hutchings, and V. C. Cornell, 1998: Wind stress measurements from the open ocean corrected for airflow distortion by the ship. *J. Phys. Oceanogr.,* **28,** 1511–1526.